RSC Advances

ROYAL SOCIETY OF CHEMISTRY

www.rsc.org/advances

RSC advances

ARTICLE

Design and discovery of tyrosinase inhibitors based on the coumarin scaffold

Received 00th January 20xx,
Accepted 00th January 20xx

DOI: 10.1039/x0xx00000x

www.rsc.org/

M. J. Matos,[a,b,*] C. Varela,[c] S. Vilar,[b,d] G. Hripcsak,[d] F. Borges,[a] L. Santana,[b] E. Uriarte,[b] A. Fais,[e] A. Di Petrillo,[e] F. Pintus[e] and B. Era[e]

Corresponding Author * Tel: +351 220 402 653; e-mail: mariacmatos@gmail.com

In this manuscript we report the synthesis, pharmacological evaluation and docking studies of a selected series of 3-a and 3-heteroarylcoumarins with the aim of finding structural features for the tyrosinase inhibitory activity. The synthesized compounds were evaluated as mushroom tyrosinase inhibitors. Compound **12b** showed the lowest IC_{50} (0.19 µM) of the series, being approximately 100 times more active than kojic acid, used as reference compound. The kinetic studies of tyrosinase inhibition revealed that **12b** acts as a competitive inhibitor of mushroom tyrosinase with L-DOPA as the substrate. Furthermore, it was determined the absence of cytotoxicity in B16F10 melanoma cells for this compound. The antioxidant profile of all the derivatives was evaluated by measuring radical scavenging capacity (ABTS and DPP assays). Docking experiments were carried out on mushroom tyrosinase structure to better understand the structure–activity relationships

Introduction

Tyrosinase (EC 1.14.18.1) is a dinuclear copper-containing multifunctional enzyme widely distributed in nature.[1] Tyrosinase oxidizes phenols and diphenols using a catalytic mechanism that depends on the presence of copper at its active site.[2] This enzyme catalyzes both initial reactions in melanogenesis: the hydroxylation of tyrosine to form L-DOPA and the subsequent oxidation of L-DOPA into dopaquinone.[3] Tyrosinase is mainly involved in the synthesis of melanin, and other polyphenolic compounds, in the skin and hair as well as neuromelanin in the brain.[4] In fact, tyrosinase inhibitors have been used as depigmenting agents for the treatment or prevention of hyperpigmentation disorders.[5] Also, tyrosinase is involved in the process to maintain the appearance, flavour, texture and nutritional value of many fresh-cut products.[6] The enzyme extracted from the mushroom *Agaricus bisporus* (*A. bisporus*) has high homology with the mammalian one.[7] So, it is suited as a model for melanogenesis and tyrosinase bio-pathways studies.[8]

Tyrosinase inhibitors have a huge importance in medicine, cosmetics and agriculture.[9,10] A great amount of research performed in this area is related with the tyrosinase inhibitory activity of plant extracts, not isolated compounds.[11] Although many tyrosinase inhibitors are available, they have demonstrated only mild efficacy and safety concerns. Therefore, from the current arsenal of compounds, none, as of yet, have reached the potency and safety requirements needed to enter clinical trials.[12] This has led to a safer, more potent and efficient discovery of novel tyrosinase inhibitors.[13] The emergence of new *in vitro* and *in vivo* tests will finally allow the arrival of new compounds with more potency and potential interest in this field.

A large number naturally occurring compounds has been reported as moderate to potent inhibitors of tyrosinase.[14,15] Among them, phenolic compounds, in particular polyphenols, were reported to have many human health benefits, including tyrosinase inhibitory activity.[16,17] Many flavonoid derivatives have been revealed to be the strongest inhibitors of tyrosinase.[18] In recent studies, some coumarins proved to be mushroom tyrosinase inhibitors.[19,20,21] In the work of Masamoto *et al.*, esculetin (IC_{50} = 43 µM) and umbelliferone (IC_{50} = 420 µM) (Figure 1A) proved to be some of the best tyrosinase inhibitors, exhibiting esculetin the strongest inhibitory activity of the entire series.[22] Liu *et al.* reported that 2-(1-(coumarin-3-yl)ethylidene)hydrazinecarbothioamide (Figure 1A) exhibited the most potent tyrosinase inhibitory activity of the studied series, with IC_{50} value of 3.44 µM.[20]

[a] CIQUP/Department of Chemistry and Biochemistry, Faculty of Sciences, University of Porto, 4169-007 Porto, Portugal
[b] Department of Organic Chemistry, Faculty of Pharmacy, University of Santiago de Compostela, 15782 Santiago de Compostela, Spain
[c] CNC-IBILI, Pharmaceutical Chemistry Group, Faculty of Pharmacy, University of Coimbra, 3000-548 Coimbra, Portugal
[d] Department of Biomedical Informatics, Columbia University Medical Center, New York, NY 10032, USA
[e] Department of Life Science and Environment, University of Cagliari, 09042 Monserrato, Cagliari, Italy

Electronic Supplementary Information (ESI) available: [details of any supplementary information available should be included here]. See DOI: 10.1039/x0xx00000x

Recently, and in contrast with the Masamoto's findings, Sollai *et al.* have shown that esculetin is considered a tyrosinase substrate rather than an inhibitor, whereas umbelliferone seems to be an inhibitor of the mentioned oxidase.[23] Structural modifications on the coumarin scaffold have become a powerful tool on tyrosinase inhibitors drug discovery.[24] One of the best strategies was the introduction of hydroxyl groups in different positions of the coumarin core (Figure 1A).[21,25,26] In addition, 4-(6-hydroxy-2-naphthyl)-1,3-bezendiol (Figure 1B) proved to be a potent tyrosinase inhibitor (IC_{50} = 0.07 μM).[27] Finally, kojic acid (used as reference compound) is a flavonoid structurally related to the 3-arylcoumarin.[27] This compound is also tyrosinase inhibitor (IC_{50} = 38.24 μM).[27]

These previous studies proved that both simple hydroxycoumarins and multi-hydroxylated 3-arylcoumarins were interesting scaffolds to further modulate the tyrosinase inhibitory activity. Further, a modification of phenyl rings by other heterocyclic rings (i.e. thiophenyl rings) is a common approach in Medicinal Chemistry (Figure 1C).

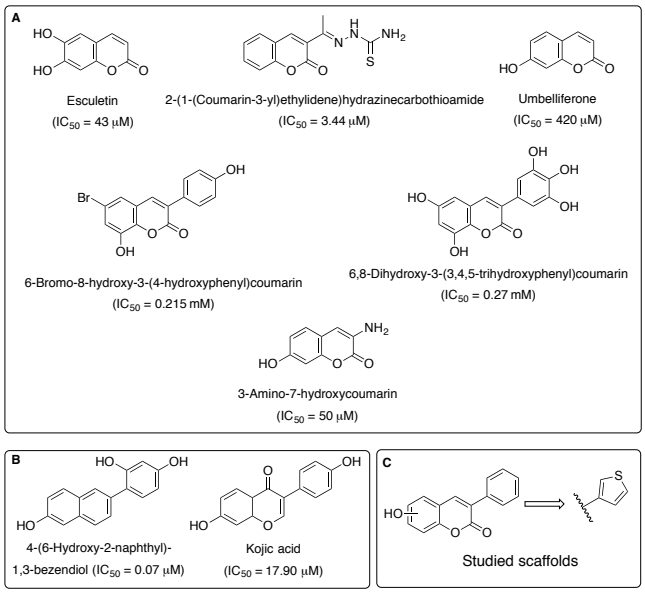

Figure 1. A – Reference inhibitors and previously described compounds bearing the coumarin scaffold; **B –** 4-(6-Hydroxy-2-naphthyl)-1,3-bezendiol and Kojic acid; **C –** Scaffolds studied in the current work.

Recent evidences have shown the importance of the antioxidant activity displayed by compounds with other pharmacological activities, such as tyrosinase inhibition.[28,29] In addition, tyrosinase inhibitors could have broad applications in therapeutics. As the ideal drug candidate has not been attained, an intensive search for new and innovative tyrosinase inhibitors is still needed. In this context, and in an attempt to develop novel tyrosinase inhibitors, in the current work we described the synthesis, biological evaluation (tyrosinase inhibitory activity, antioxidant activity and cytotoxicity in melanoma cells) and docking calculations of the selected 3-aryl and 3-heteroarylcoumarins. This paper emphasizes the rationale behind the discovery of tyrosinase inhibitors bearing the coumarin scaffold, the study of structure–activity relationships based on theoretical calculations, mechanisms and kinetic of inhibition and the effect of the inhibitors on the viability of mice melanoma cells (B16F10).

Experimental

Materials and methods

Chemistry

Starting materials and reagents were obtained from commercial suppliers (Sigma-Aldrich) and were used without further purification. Melting points (mp) are uncorrected and were determined with a Reichert Kofler thermopan or in capillary tubes in a Büchi 510 apparatus. ^{1}H NMR (300 MHz) and ^{13}C NMR (75.4 MHz) spectra were recorder with a Bruker AMX spectrometer using DMSO-d_6 as solvent. Chemical shifts (δ) are expressed in parts per million (ppm) using TMS as an internal standard. Coupling constants *J* are expressed in Hertz (Hz). Spin multiplicities are given as s (singlet), d (doublet), dd (doublet of doublets) and m (multiplet). Mass spectrometry was carried out with a Hewlett-Packard 5988A spectrometer. Elemental analyses were performed by a Perkin-Elmer 240B microanalyzer and are within ±0.4% of calculated values in all cases. The analytical results are ≥ 98% purity for all compounds. Flash chromatography (FC) was performed on silica gel (Merck 60, 230-400 mesh); analytical TLC was performed on precoated silica gel plates (Merck 60 F254). Organic solutions were dried over anhydrous sodium sulfate. Concentration and evaporation of the solvent after reaction or extraction was carried out on a rotary evaporator (Büchi Rotavapor) operating under reduced pressure.

Mass, ^{1}H and ^{13}C NMR spectra of the studied compounds are presented in Supplementary Information.

General procedure for the synthesis of 3-phenylcoumarin and 3-thiophenylcoumarin (1 and 7).

N,N'-Dicyclohexylcarbodiimide (11.46 mmol) was added to a solution of *ortho*-hydroxybenzaldehyde (7.34 mmol) and phenyl/thiophenylacetic acid (9.18 mmol) in dimethyl sulfoxide (15 mL). The mixture was heated at 110 °C for 24 h. Then, ice (100 mL) and acetic acid (10 mL) were added to the reaction mixture. After keeping it at room temperature for 2 h, the mixture was extracted with ether (3 x 25 mL). The organic layers were combined and washed with sodium bicarbonate solution (50 mL, 5%) and water (20 mL). Subsequently, the solvent was evaporated under vacuum and the dry residue was purified by flash chromatography (hexane/ethyl acetate 9:1), to give the desired 3-phenylcoumarin or 3-thiophenylcoumarin [**1** (yield 79%)[30] or **7** (yield 83%)[31]].[32]

General procedure for the synthesis of acetoxy-3-aryl/heteroarylcoumarins (2a-6a and 13a-15a/8a-12a).

Compound **2a**-**6a** and **13a**-**15a**/**8a**-**12a** were synthesized under anhydrous conditions, using material previously dried at 60 °C for at least 12 h and at 300 °C during few minutes immediately before use. A solution containing anhydrous CH_3CO_2K (2.94 mmol), the corresponding phenylacetic acid (for compounds

2a-**6a** and **13a**-**15a**) or thiophenylacetic acid (for compounds **8a**-**12a**) (1.67 mmol) and the corresponding hydroxysalicylaldehyde (1.67 mmol), in Ac_2O (1.2 mL), was refluxed for 16 h. The reaction mixture was cooled, neutralized with 10% aqueous $NaHCO_3$, and extracted with EtOAc (3 x 30 mL). The organic layers were combined, washed with distilled water, dried (anhydrous Na_2SO_4), and evaporated under reduced pressure. The product was purified by recrystallization in EtOH and dried, to afford the desired compound.

General procedure for the synthesis of hydroxy-3-aryl/heteroarylcoumarins (2b-6b and 13b-15b/8b-12b).
Compounds **2b**-**6b**[33,34,35,36,37] and **13b**-**15b**/**8b**-**15b** were obtained by hydrolysis of their acetoxylated counterparts **2a**-**6a** and **13a**-**15a**/**8a**-**12a**, respectively.[38,39] In general, the appropriate acetoxylated coumarin, mixed with 2 N aqueous HCl and MeOH, was refluxed during 3 h. The resulting reaction mixture was cooled in an ice-bath and the reaction product, obtained as solid, was filtered, washed with cold distilled water, and dried under vacuum, to afford the desired compound.

6-Hydroxy-3-(3-thiophenyl)coumarin (8b). Yield 92%. Mp: 263-4 °C. ^{1}H NMR (300 MHz, DMSO-d_6) δ: 7.01 (d, 1H, *J* = 2.8, H-5), 7.06 (dd, 1H, *J* = 9.0, *J* = 2.8, H-7), 7.27 (d, 1H, *J* = 8.8, H-8), 7.65 (dd, 1H, *J* = 5.0, *J* = 2.9, H-5'), 7.71 (dd, 1H, *J* = 5.2, *J* = 1.3, H-4'), 8.23 (dd, 1H, *J* = 2.9, *J* = 1.2, H-2'), 8.42 (s, 1H, H-4), 9.78 (s, 1H, OH). ^{13}C NMR (75.4 MHz, DMSO-d_6) δ: 112.4, 116.9, 119.8, 120.0, 121.5, 125.7, 126.4, 127.1, 134.9, 137.4, 138.5, 145.9, 154.0. MS *m/z*: 245 ([M+1]$^+$, 29). Anal. Elem. Calc. for $C_{17}H_{12}O_6S$: C, 63.92; H, 3.30. Found: C, 63.90; H, 3.27.

8-Hydroxy-3-(3-thiophenyl)coumarin (10b). Yield 88%. Mp: 208-9 °C. ^{1}H NMR (300 MHz, DMSO-d_6) δ: 7.04-7.17 (m, 3H, H-5', H-6, H-7), 7.62-7.71 (m, 2H, H-2', H-4'), 8.24 (dd, 1H, *J* = 7.5, *J* = 1.6, H-5), 8.43 (s, 1H, H-4), 10.25 (s, 1H, OH). ^{13}C NMR (75.4 MHz, DMSO-d_6) δ: 117.9, 118.0, 118.5, 118.6, 124.6, 124.8, 125.7, 126.4, 127.0, 139.0, 142.9, 144.5, 153.1. MS *m/z*: 245 ([M+1]$^+$, 26). Anal. Elem. Calc. for $C_{13}H_8O_3S$: C, 63.92; H, 3.30. Found: C, 63.91; H, 3.28.

5,7-Dihydroxy-3-(3-thiophenyl)coumarin (12b). Yield 92%. Mp: 315-6 °C. ^{1}H NMR (300 MHz, DMSO-d_6) δ: 6.23 (d, 1H, *J* = 2.0, H-8), 6.29 (d, 1H, *J* = 2.0, H-6), 7.51-7.63 (m, 2H, H-2', H-5'), 8.00-8.12 (m, 1H, H-4'), 8.27 (s, 1H, H-4), 10.44 (s, 1H, OH), 10.77 (s, 1H, OH). ^{13}C NMR (75.4 MHz, DMSO-d_6) δ: 93.8, 98.5, 102.2, 105.4, 123.7, 126.2, 126.7, 134.0, 135.4, 140.7, 155.4, 156.3, 162.1. MS *m/z*: 261 ([M+1]$^+$, 20). Anal. Elem. Calc. for $C_{13}H_8O_4S$: C, 59.99; H, 3.10. Found: C, 60.00; H, 3.12.

5,7-Dihydroxy-3-(3'-hydroxyphenyl)coumarin (13b). Yield 93%. Mp: 276-7 °C. ^{1}H NMR (300 MHz, DMSO-d_6) δ: 6.21-6.27 (m, 2H, H-6, H-8), 6.71-6.79 (m, 1H, H-4'), 7.02-7.23 (m, 3H, H-2', H-5', H-6'), 8.00 (s, 1H, H-4), 9.51 (s, 1H, OH), 10.38 (s, 1H, OH), 10.75 (s, 1H, OH). ^{13}C NMR (75.4 MHz, DMSO-d_6) δ: 93.8, 102.4, 113.2, 115.2, 119.8, 120.3, 120.9, 129.4, 131.2, 136.7, 138.0, 156.3, 157.2, 162.2, 172.1. MS *m/z*: 270 ([M+1]$^+$, 100). Anal. Elem. Calc. for $C_{15}H_{10}O_5$: C, 66.67; H, 3.73;. Found: C, 66.65; H, 3.70.

5,7-Dihydroxy-3-(3',4'-dihydroxyphenyl)coumarin (14b). Yield 88%. Mp: 336-7 °C. ^{1}H NMR (300 MHz, DMSO-d_6) δ: 6.18-6.22 (m, 2H, H-6, H-8), 6.74 (d, 2H, *J* = 8.2, H-6'), 6.94 (dd, 1H, *J* = 8.2, *J* = 2.1, H-5'), 7.10 (d, 1H, *J* = 2.1, H-2'), 7.90 (s, 1H, H-4), 9.12 (s, 2H, OH), 10.31 (s, 1H, OH), 10.64 (s, 1H, OH). ^{13}C NMR (75.4 MHz, DMSO-d_6) δ: 93.7, 98.4, 102.5, 115.5, 115.7, 119.4, 119.5, 199.5, 119.9, 126.6, 134.0, 144.9, 145.6, 155.9, 161.6. MS *m/z*: 286 ([M+1]$^+$, 10). Anal. Elem. Calc. for $C_{15}H_{10}O_6$: C, 62.94; H, 3.52. Found: C, 62.97; H, 3.52.

3-(4'-Bromophenyl)-5,7-dihydroxycoumarin (15b). Yield 90%. Mp: 288-9 °C. ^{1}H NMR (300 MHz, DMSO-d_6) δ: 6.21-6.29 (m, 2H, H-6, H-8), 7.54-7.63 (m, 4H, H-2', H-3', H-5', H-6'), 8.09 (s, 1H, H-4), 10.43 (s, 1H, OH), 10.75 (s, 1H, OH). ^{13}C NMR (75.4 MHz, DMSO-d_6) δ: 99.2, 103.8, 107.8, 123.7, 126.4, 135.6, 136.5, 140.1, 141.6, 161.3, 161.8, 165.5, 167.8. MS *m/z*: 333 ([M+1]$^+$, 100). Anal. Elem. Calc. for $C_{15}H_9BrO_4$: C, 54.08; H, 2.72. Found: C, 54.04; H, 2.70.

Pharmacology

Tyrosinase inhibition assay

Tyrosinase inhibition assay was carried out using the following protocol. Briefly, in a 96-well plate, 80 µL of phosphate buffer (0.5 M, pH 6.5), 60 µL of mushroom tyrosinase (240 UmL^{-1}), 20 µL of inhibitor dissolved in DMSO at the desired concentrations or DMSO (control), were mixed. The assay mixture was then incubated at 37 °C for 10 min. Finally, 40 µL of 2.5 mM L-DOPA in phosphate buffer were added and immediately monitored (t = 0) at 492 nm for dopachrome formation in the reaction mixture.

Kojic acid was used as a positive control. Each measurement was made at least in triplicate. The percentage of inhibition of tyrosinase activity was calculated as inhibition (%) = (A-B)/A×100, where A represents the difference in the absorbance of control sample between an incubation time of 0.5 and 1.0 min, and B represents the difference in absorbance of the test sample between an incubation time of 0.5 and 1.0 min. The IC_{50} value, a concentration giving 50% inhibition of tyrosinase activity, was determinate by interpolation of dose-response curves.

The mode of inhibition on the enzyme was performed using the Lineweaver-Burk plot. Different concentrations of L-DOPA (0.3, 0.5, 0.7 and 1.0 mM) were used for the assay.

Determination of copper chelation

The copper chelating capacity of the compound **12b** and **15b** was determined by the UV/Vis spectra according to the protocol described by Kubo *et al.*[40] The compounds (0.05 mM) were mixed with different concentration of $CuSO_4$ (0.025-0.1 mM) and, after incubation at 25 °C for 10 min, absorption spectra from 200 to 800 nm was recorded.

For determination of the ability of compound **12b** and **15b** to chelate copper in the enzyme, the mixture of 1.8 mL of 0.1 M phosphate buffer (pH 6.8), 1 mL of water, 0.1 mL of the sample

solution (0.05 mM) and 0.1 mL of the aqueous solution of the mushroom tyrosinase (50 units), was incubated at 25 °C for 30 min, and then UV-Vis spectra were recorded.

Antioxidant activity

Total free radical-scavenging capacity of the molecules presenting hydroxyl groups on their structure was determined by $ABTS^{\cdot+}$ and $DPPH^{\cdot}$ scavenging methods, using trolox as antioxidant standard.

ABTS radical scavenging activity

The $ABTS^{\cdot+}$ method is based on the capacity of an antioxidant to scavenge the free $ABTS^{\cdot+}$ and was performed as previously reported.[41] $ABTS^{\cdot+}$ reagent was produced by reacting 7 mM ABTS with 2.45 mM potassium persulfate (final concentration) in aqueous solution. The mixture was kept in the dark, at room temperature, for 24 h. The concentration of the blue-green $ABTS^{\cdot+}$ solution was adjusted to an absorbance of 0.700 ± 0.02 (mean ± SD) at 734 nm.

The samples of the compounds (10 µL) were added to $ABTS^{\cdot+}$ solution and incubated in the dark at room temperature for 1 min. Afterwards the decrease in A734 was calculated and referred to the trolox standard curve. The activity was expressed as concentration of sample necessary to give a 50% reduction in the original absorbance (EC_{50}).

DPPH radical scavenging activity

The $DPPH^{\cdot}$ scavenging activity of the compounds was analyzed according to the procedure previously described.[42] Each compound, in DMSO solution (20 µL), was added to a mixture of 100 mM acetate buffer (pH 6.5, 630 µL) and 0.3 mM DPPH in ethanol (350 µL) in a cuvette, and left at room temperature, in the dark, for 15 min. The absorbance of the resulting solutions was measured at 515 nm. Scavenging capacity of each sample was compared to that of DMSO (0% radical scavenging) and trolox (positive control, 100% radical scavenging). The results were expressed as concentration of the compounds capable of scavenging 50% of free radicals (EC_{50}).

Cell viability

Murine melanoma B16F10 cells (CRL-6475) were purchased from the American Type Culture Collection (ATCC, Manassas, VA, USA). The cells were cultured in Dulbecco's Modified Eagle Medium (DMEM) containing 10% fetal bovine serum (FBS, Gibco, NY, USA), and 1% penicillin/streptomycin at 37 °C in a humidified atmosphere with 5% CO_2.

Cell viability was detected by the colorimetric 3-(4,5-dimethylthiazol-2-yl)-2,5-diphenyltetrazolium bromide (MTT) assay.[43] Briefly, cells were seeded in a 96-well plate (10^4 cells/well) and exposed to compound **12b** or **15b** at different concentrations (5-100 µM). After 48 h of incubation, cells were labelled with MTT solution for 3 h at 37 °C. The resulting violet formazan precipitate was dissolved in isopropanol and the absorbance of each well was determined at 590 nm, using a microplate reader with a 630 nm reference.

Molecular Docking

Docking calculations were performed with Glide from the Schrödinger package.[44]

Ligands and protein preparation: Ligands were pre-processed with the LigPrep module[44] that generated tautomers, different protonation states (pH = 7.0 ± 2.0) and optimized the molecular structures with OPLS_2005 force field. Crystallized proteins selected to run the calculations were 2Y9W (PDB code)[45] and 2Y9X,[45] extracted from the organism *A. bisporus*. A water molecule or hydroxyl ion is present in the 2Y9W protein pocket coordinated with Cu^{2+}. The hydroxyl ion is maintained in the pocket for the docking calculations. On the other hand, the crystal structure 2Y9X represents the deoxy form of the enzyme. The Protein Preparation Workflow[44] was used to treat the proteins. As an example, some steps described in the workflow included: addition and optimization of hydrogens and the hydrogen bonding network, addition of cap termini, optimization of protonation states of some residues (His, Asp and Glu), among others.

Molecular docking calculation: In the first step, we calculated a receptor grid centered in the pocket, with a van der Waals radii scaling factor of 1.0 and a partial atomic charge cut-off of 0.25. In the second step, we docked the compounds to the tyrosinase crystal structure 2Y9W and 2Y9X[44] using Glide SP (standard precision) and XP (extra-precision). The final binding mode described in the manuscript was selected taking into account the best-ranked scoring functions.

Results and discussion

Chemistry

Compounds **1**, **7** and **2b**-**6b** and **8b**-**12b** were efficiently synthesized according to the synthetic strategy outlined in Scheme 1. Compound **1** and **7** are obtained by a Perkin reaction, starting from the commercially available *ortho*-hydroxybenzaldehyde and the phenyl/2-(thiophen-3-yl)acetic acid, using *N,N'*-dicyclohexylcarbodiimide (DCC) as dehydrating agent, and DMSO as solvent, at 110 °C.[32] The synthetic methodology to obtain **2b**-**6b** and **8b**-**12b** occurs in two different steps. The first one is a Perkin-Oglialoro condensation of different commercially available hydroxybenzaldehydes and aryl/heteroarylacetic acids, using potassium acetate (CH_3CO_2K) in acetic anhydride (Ac_2O), under reflux, for 16 h, to obtain the acetoxy-3-aryl/heteroarylcoumarins (**2a**-**6a** and **8a**-**12a**). Acetylation of the hydroxyl groups and pyrone ring closure occurred simultaneously. The second step is a hydrolysis of the obtained acetoxy derivatives, in the presence of aqueous HCl solution and MeOH, under reflux, for 3 h, to achieve the hydroxyl substituted 3-aryl/heteroarylcoumarins (**2b**-**6b** and **8b**-**12b**).[46] Structures of the synthesized compounds were established on the basis of their spectral data (see Experimental Section).

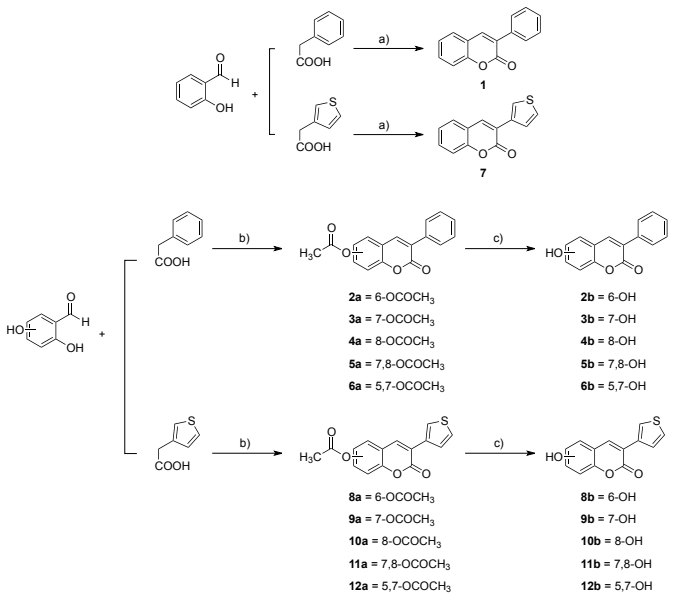

Scheme 1. Synthetic methodologies. Reagents and conditions: a) DCC, DMSO, 110 °C, 24 h; b) CH_3CO_2K, Ac_2O, reflux, 16 h; c) HCl, MeOH, reflux, 3 h.

After the biological studies, and the excellent inhibitory and antioxidant profile of compounds **6b** and **12b**, a selected series with structural variability at position 3, maintaining the phenolic hydroxyls present in the coumarin skeleton (compounds **13b**-**15b**) were efficiently synthesized according to the synthetic strategy outlined in Scheme 2. As described before, the synthetic methodology occurs in two different steps: i) Perkin-Oglialoro condensation of different commercially available hydroxybenzaldehydes and arylacetic acids to obtain the acetoxy-3-arylcoumarins (**13a**-**15a**) ii) and hydrolysis of the obtained acetoxy derivatives to achieve the hydroxyl substituted 3-aryl/heteroarylcoumarins (**13b**-**15b**). Structures of the synthesized compounds were established on the basis of their spectral data (see Experimental Section).

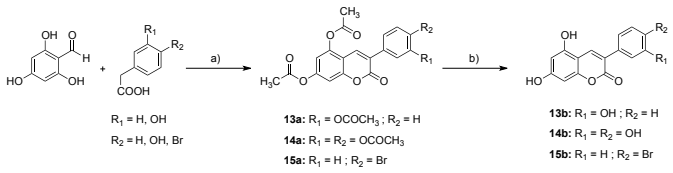

Scheme 2. Synthetic methodologies. Reagents and conditions: a) CH_3CO_2K, Ac_2O, reflux, 16 h; b) HCl, MeOH, reflux, 3 h.

Pharmacology

In vitro tyrosinase inhibition

The tyrosinase inhibitory activity of all the synthetized compounds was evaluated in vitro by the measurement of the enzymatic activity of tyrosinase enzyme extracted from the mushroom species *A. bisporus*. The compounds were screened for *o*-diphenolase inhibitory activity of tyrosinase, using L-DOPA as substrate. The IC_{50} values of all compounds and reference inhibitor, kojic acid, are summarized in Table 1.

Table 1. IC_{50} values of 3-aryl and 3-heteroarylcoumarins in mushroom tyrosinase activity.

Compounds	IC_{50} (μM)[a]
1	> 1000
2b	300.0 ± 25.95
3b[25]	> 1000
4b[26]	> 1000
5b	> 1000
6b	408.37 ± 19.66
7	> 1000
8b	> 1000
9b	821.65 ± 137.45
10b	> 1000
11b	508.75 ± 4.83
12b	0.19 ± 0.016
13b	727.05 ± 3.05
14b	376.02 ± 0.008
15b	1.05 ± 0.056
Kojic acid[b]	17.90 ± 0.98

[a] Values were shown as Mean ± SE (n = 3)

[b] Positive control

As shown in Table 1, from the studied series, compounds **2b**, **6b**, **9b** and **11b**-**15b** displayed inhibitory activity. Compounds **12b** (IC_{50} = 0.19 μM) and **15b** (IC_{50} = 1.05 μM) were better tyrosinase inhibitors than the reference compound, kojic acid (IC_{50} = 17.9 μM). In fact, compound **12b** proved to be approximately 100 times more active than kojic acid.

Compounds **1** and **7**, the studied scaffolds without substituents, proved to be inactive at the highest tested concentration. Compounds **3b** and **4b** were already described for their tyrosinase activity in previous papers.[25,26] They were included in this manuscript due to their interest to complete the structure-activity relationship study.

In general, the most relevant structural feature for the activity of both series of compounds (3-phenyl and 3-thiophenyl derivatives), is the presence of two hydroxyl groups at positions 5 and 7 of the coumarin moiety, as all these compounds (**6b** and **12b**-**15b**) were active against the studied target.

The mode of inhibition of the enzyme was determined by Lineweaver-Burk plot analysis, as shown in Figures 2 and 3. Plots of the initial rates of tyrosinase activity in the presence of increasing concentrations of substrate yielded a family of straight lines with different slopes but they intersected one another on the Y-axis, which indicates that compound **12b** is a competitive inhibitor (Figure 2a). The inhibition constant (Ki) for the inhibitor binding with the free enzyme (E) was obtained from the secondary plot as 0.22 µM (Figure 2b).

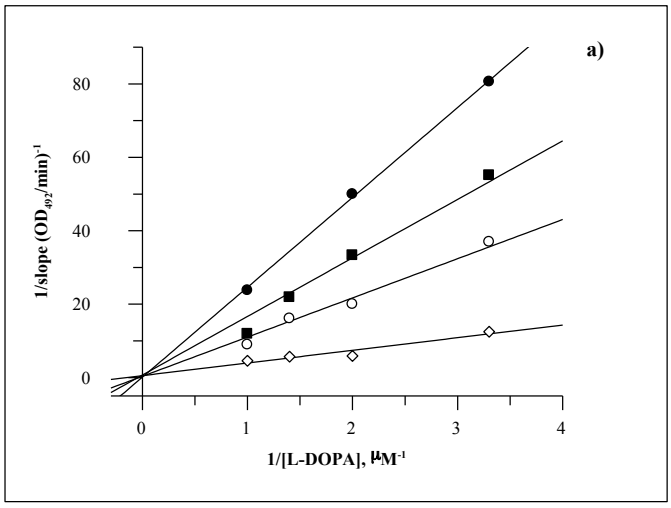

Figure 2. a) Lineweaver–Burk plots for the inhibition of compound **12b** on mushroom tyrosinase for catalysis of L-DOPA. The concentrations of inhibitor were 0 (◊), 0.25 (○), 0.5 (▪) and 1.0 (●) µM. b) The secondary plot of slope (K_m/V_{max}) *versus* concentration of compound **12b**, to determine the inhibition constant (K_i).

In the presence of **15b**, the Lineweaver–Burk plots (Figure 3) showed that this compound was a mixed-type inhibitor since increasing the concentration of **15b** resulted in a family of straight lines with different slope and y-intercepts, which intersected in the second quadrant. This behaviour demonstrated that compound **15b** can bind not only with the free enzyme, but also with the enzyme-substrate complex, and their equilibrium constants are different. The equilibrium constants for inhibitor binding with the free enzyme (K_I) and with the enzyme-substrate complex (K_{IS}) were obtained from the slope or the vertical intercept *versus* inhibitor concentration, respectively (data presented in Supplementary Information). The values of K_I and K_{IS} of compound **15b** were determined to be 0.89 and 5.38 µM, respectively.

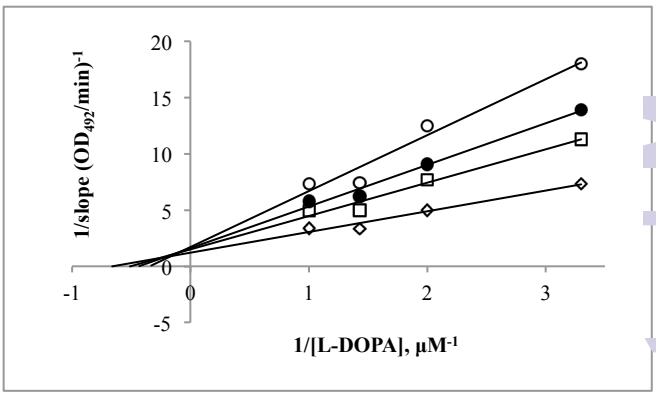

Figure 3. Lineweaver–Burk plots for the inhibition of compound **15b** on mushroom tyrosinase for catalysis of L-DOPA. The concentrations of inhibitor were 0 (◊), 0.5 (□), 1.0 (●), and 1.5 (○) µM.

Tyrosinase inhibitors might exert their effect by chelating copper ion in the active site of the enzyme. In order to determine whether the inhibitory activity of the compounds **12b** and **15b** are dependent on the ability to chelate the copper ions, tests with copper sulfate or mushroom tyrosinase were carried out. A solution of the compound **12b** or **15b** (50 µM) in phosphate buffer was scanned with and without copper sulfate (up to 500 µM) or tyrosinase (50 units), and the spectra obtained were compared. UV-Vis spectra showed no significant change by adding Cu^{2+} or by incubation with the enzyme. Thus, no interaction between compounds and copper was observed.

Antioxidant assays

Radical scavengers can protect the biosynthesis and food browning process. They are also involved in non-enzymatic oxidation, as well as its oxidation process. Therefore, in the present study, antioxidant activity of the hydroxylated compounds was evaluated by measuring radical scavenging capacity (ABTS and DPPH assays). The results are summarized in Table 2.

Table 2. EC_{50} values of selected 3-aryl and 3-heteroarylcoumarins (**2b**-**15b**).

Compound	EC_{50} (μM)[a]	
	ABTS	DPPH
2b	177.7 ± 1.85	161.81 ± 2.57
3b	> 300	> 300
4b	63.44 ± 1.33	223.07 ± 5.38
5b	11.59 ± 0.39	11.39 ± 0.24
6b	7.08 ± 0.035	6.30 ± 3.82
8b	> 600	> 300
9b	> 600	> 300
10b	> 600	> 300
11b	10.15 ± 1.20	7.71 ± 0.09
12b	8.40 ± 0.28	9.42 ± 0.31
13b	8.62 ± 0.18	15.54 ± 0.19
14b	5.46 ± 0.85	11.64 ± 1.00
15b	20.77 ± 0.42	18.65 ± 0.85
Trolox[b]	5.28 ± 0.15	28.27 ± 0.45

[a] The EC_{50} value is the concentration of antioxidant required to quench 50% of the radicals in the reaction mixture under the experimental conditions. Each EC_{50} value is the mean ± SEM from three experiments (n = 3).

[b] Positive control

As shown in Table 2, compounds that incorporate a single hydroxyl group on their structure (compounds **2b**-**4b** and **8b**-**10b**) did not present effective radical and radical cation scavenging activity, measured in both ABTS and DPPH methods. In particular, compounds **3b** and **8b**-**10b** proved to be inactive at the highest tested concentration in both assays.

The best compounds, due to their capacity to scavenging both radicals ($ABTS^{\cdot+}$ and $DPPH^{\cdot}$) proved to be compounds **5b**, **6b** and **11b**-**14b**. Regarding the $DPPH^{\cdot}$ scavenging capacity, these compounds exhibited higher activity than trolox, with EC_{50} values ranged from 6.30 to 15.54 μM. Among the different tested coumarins, compound **6b** (EC_{50} = 6.30 μM) exhibited the most potent $DPPH^{\cdot}$ scavenging activity, being this compound about 5 times more potent than standard (trolox, EC_{50} = 28.27 μM). Regarding the $ABTS^{\cdot+}$ assay, the highlighted compounds showed EC_{50} values ranged from 7.08 to 11.59 μM, being compounds **6b**, **12b**, **13b** and **14b** in the same range (EC_{50} = 7.08, 8.40, 8.62 and 5.46 μM, respectively) than trolox (EC_{50} = 5.28 μM).

Taking into account these results, and the structural characteristics of the compounds, it could be observed that the presence of two hydroxyl groups in the coumarin scaffold, either in the positions 5/7 or in the positions 7/8, seems to be important for the desired antioxidant activity.

Effect of the compound 12b and 15b on the viability of B16F10 melanoma cells

The cytotoxicity of compound **12b**, which showed the strongest mushroom tyrosinase inhibition (IC_{50} = 0.19 μM), was carried out to determine the safety of this molecule (Figure 4a). Cells were treated with different concentration of compound (5–100 μM) for 48 h and were examined using MTT test. The results indicate that this inhibitor exhibited no considerable cytotoxic effect in B16F10 melanoma cells at the concentration in which inhibits the tyrosinase activity. The same protocol was applied for compound **15b**, which proved to be a very good tyrosinase inhibitor (IC_{50} = 1.05 μM). A similar result was obtained: the compound proved to be non-cytotoxic to the cells under the experimental conditions (Figure 4b).

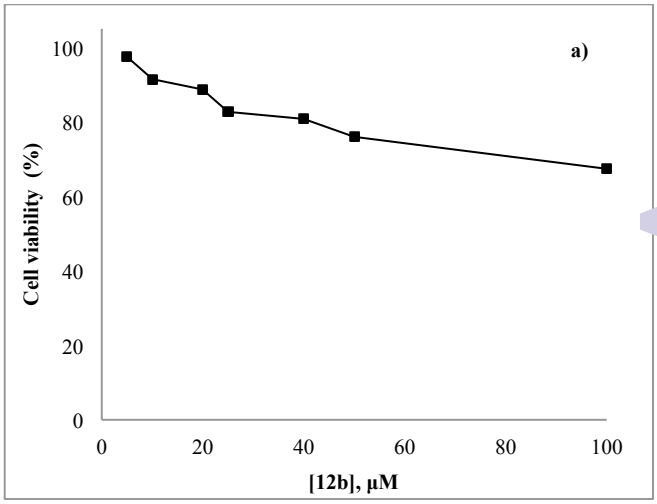

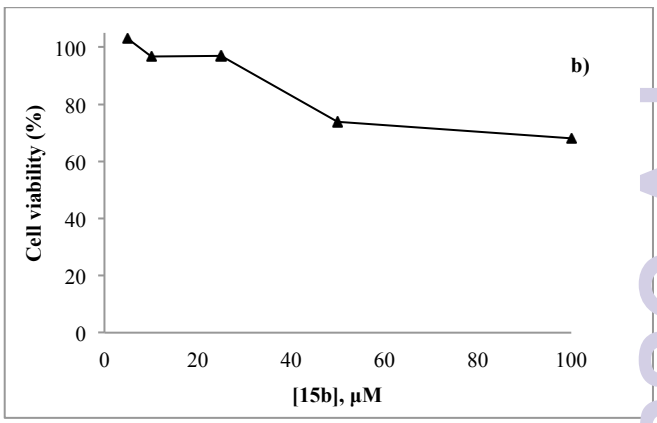

Figure 4. The effect of inhibitors on B16F10 cell viability. a) compound **12b**; b) compound **15b**. Cells were treated with different concentrations of compound (5-100 μM) and studied by MTT assay. Data are expressed as a percentage of the control.

Docking calculations

Some compounds shown in Scheme 1 were studied with molecular docking techniques to understand the possible key interactions responsible for the protein-ligand binding. We used the crystal structure 2Y9W (PDB code)[45] in which the crystallized tyrosinase belongs to the mushroom *A. bisporus*, the same organism used in our experimental in vitro tyrosinase inhibition. No ligand is present in the active site of the crystallized enzyme. The protein structure contains a water molecule or hydroxyl ion coordinated with the copper ions. We considered the oxy form of the enzyme as a suitable template for docking calculations. Moreover, an additional docking using the structure 2Y9X (PDB code),[45] representing the deoxy state of the enzyme, was performed to evaluate the stability of the results. The ligands were docked to the protein through Glide in the Schrodinger package.[44] With the aim of validating our docking protocol, we measured the root mean square deviation (RMSD) between the atomic coordinates of the co-crystallized and the theoretical pose of the tropolone inhibitor present in the 2Y9X. The crystal structure (2Y9X) is a tetramer with tropolone bound to different subunits with a slight different conformation depending on the subunit. Docking simulations reproduced the best X-ray crystal parameters with a RMSD of 1.24 and 2.30 Å using the protein structures 2Y9W and 2Y9X respectively (see Figure 5a with the co-crystallized tropolone in the 2Y9X structure). In the case of 2Y9W the protein was superimposed to 2Y9X and the RMSD between the co-crystallized tropolone in 2Y9X and the theoretical pose determined in 2Y9W was measured.

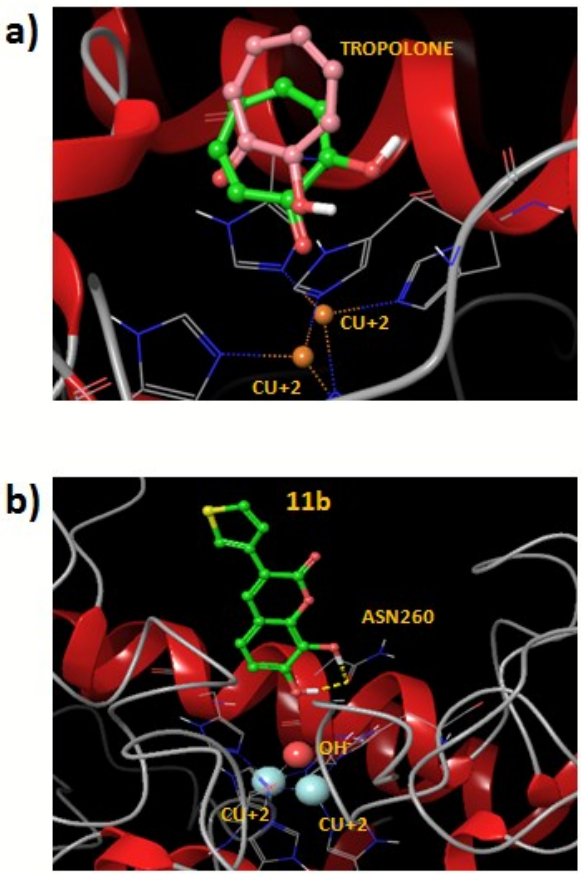

Figure 5. a) Comparison of the co-crystallized ligand tropolone (pink color) and the binding mode calculated with the molecular docking (green color) in the tyrosinase crystal structure (PDB: 2Y9X); b) Hypothetical binding mode calculated with docking for compound 11b inside the 2Y9W tyrosinase. Hydrogen bonds are represented in yellow dashed lines.

Compounds with tyrosinase activity, such as compounds **6b**, **9b**, **11b** and **12b** showed a similar binding mode inside the active site of the tyrosinase. The compounds orientated the coumarin ring towards the bottom of the cavity close to the catalytic site and the 3-aryl or heteroaryl ring towards the protein surface. The hydroxyl group at position 7 of compounds **6b**, **9b**, **11b** and **12b** established a hydrogen bond with the amide moiety of residue Asn260 (see Figure 5 and 6). Compound **11b** also established a hydrogen bond with the same residue Asn260 using the hydroxyl group at position 8 (Figure 5b). Moreover, compound **6b** and **12b** established an additional hydrogen bond with the residue Met280 using the hydroxyl group at position 5 (see Figure 6). This second stabilizing interaction could be responsible for the higher activity shown by compound **6b** compared to the other compounds in the series with 3-phenyl substitutions. Similar argument can be made to explain the improved activity shown by compound **12b** regarding the series with 3-heteroaryl substituents. On the other hand, compounds with heteroaryl moieties showed a better tyrosinase activity than compounds with 3-phenyl substituents. Increased polarity in the 3-aryl substitution that points out towards the enzyme surface seems to have an important effect in the enzyme affinity. The poses yielded by the calculations showed that the ligands orientated the 3-substitution towards a polar area defined by the Arg268, a charged residue with hydrophilic characteristics.

We also performed an alternative docking with the other available tyrosinase crystal structure from *A. bisporus* (PDB ID 2Y9X).[45] The main difference in the crystallized active site is the presence of the inhibitor tropolone and the lack of a water molecule or hydroxyl between the copper ions. Molecular docking using the 2Y9X protein yielded similar binding modes for the compounds.

To better study the interaction profile of compound **12b**, we calculated the contribution of the residues to the interaction with the ligand. Figure 6d shows the interaction score for the residues placed in a distance of 4 Å from the ligand (score is measured as the sum of Coulomb, van der Waals and hydrogen bonding contributions). The residue that contributes the most is the Asn260. The compound established Coulomb interactions mainly with residues Asn260, Gly281 and Met280. Van der Waals contributions are important in residues such as His263, Phe264, Val283 and Arg268. Our docking results are in accordance with the experimental data that showed that the ligand **12b** is a competitive inhibitor, but no interaction with the copper ions was detected.

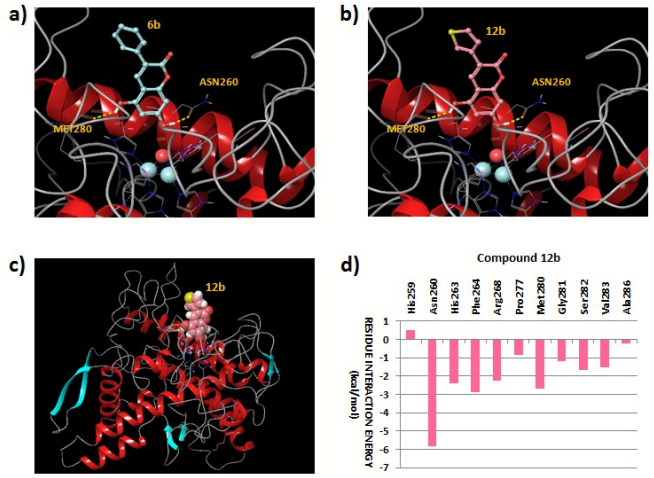

Figure 6. Pose extracted from the docking for compound **6b** (panel a) and **12b** (panel b) in the tyrosinase crystal structure (PDB: 2Y9W). Hydrogen bonds are represented in yellow color. Panel c) shows the perspective of the whole tyrosinase with the inhibitor **12b** docked to the protein. Panel d) represents the residue interaction contribution (Coulomb, van der Waals and hydrogen bonding scores) between the protein (residues selected in a distance of 4 Å from the ligand) and compound **12b**.

Conclusions

This study showed that some of the synthesized derivatives displayed inhibitory activity against mushroom tyrosinase. The two most active compounds (**12b** and **15b**) presented tyrosinase inhibitory activity in the low-micromolar range (IC_{50} = 0.19 and 1.05 µM, respectively), better than kojic acid (IC_{50} = 17.90 µM), used as reference compound. The presence of two hydroxyl groups at positions 5/7 of the coumarin scaffold improved the inhibitory activity compared to the other synthesized derivatives and the reference compound. The mode of inhibition of the enzyme was determined by Lineweaver-Burk plot analysis, and indicated that compound **12b** is a competitive inhibitor and compound **15b** is a mixed-type inhibitor. It was also proved that the inhibitory activity of both compounds is not dependent on the ability to chelate the copper ions in the active site of the enzyme. Melanoma cells are widely used as cellular models to study tyrosinase inhibitors. Both compounds also proved to exhibit no considerable cytotoxic effect in B16F10 melanoma cells at any concentration used in the study of the tyrosinase activity. The docking results were in accordance with the experimental data, which showed that the ligand **12b** is a competitive inhibitor, but no interaction with the copper ions was detected. Among the different tested coumarins, compound **12b** exhibited one of the most potent $DPPH^{\cdot}$ scavenging activity (EC_{50} = 9.42 µM), being more potent than standard (trolox, EC_{50} = 28.27 µM). Regarding the $ABTS^{\cdot+}$ assay, once again compound **12b** was one of the best compounds (EC_{50} = 8.40 µM). Therefore, the introduction of hydroxyl groups on the coumarin scaffold, as well as the substituent at position 3, seems to modulate the pharmacological potential of these coumarins, confirming that these leads could be effectively optimized in candidates for the treatment of disorders related to the melanin biosynthesis, such as hyperpigmentation skin diseases. These findings have encouraged us to continue the effort towards the optimization of the pharmacological profile of these coumarins.

Acknowledgements

This work was partially supported by University of Santiago de Compostela, University of Cagliari, Portuguese Foundation for Science and Technology (FCT) of Portugal and QREN (FCUP-CIQ-UP-NORTE-07-0124-FEDER-000065) project, European Social Fund (ESF), Angeles Alvariño program from Xunta de Galicia (Plan I2C), Galician Plan of research, innovation and growth 2011-2015 (Plan I2C - ED481B 2014/086-0) and FCT POPH and QREN (SFRH/BPD/95345/2013).

Notes and references

1 K. Lerch, *Life Chem. Rep.*, 1987, 5, 221.
2 F. Solano, S. Briganti, M. Picardo and G. Ghanem, *Pigm. Cell Res.*, 2006, **19**, 550.
3 Y.M. Kim, J. Yun, C. Lee, H. Lee, K.R. Min and Y. Kim, *J. Biol Chem.*, 2002, **277**, 16340.
4 S. Li and J.-S. Ding, *Zhongnan Yaoxue*, 2013, **11(4)**, 278.
5 T. Pillaiyar, M. Manickam and S.H. Jung, *Expert Opin. Ther. Pat.*, 2015, **25(7)**, 775.
6 L. Qiu, Q.H. Chen, J.X. Zhuang, X. Zhong, J.J. Zhou, Y.J. Guo and Q.X. Chen, *Food Chem.*, 2009, **112**, 609.
7 C. Gasparetti, E. Nordlund, J. Janis, J. Buchert and K. Kruus, *Biochim. Biophys. Acta*, 2012, **1824(4)**, 598.
8 X. Zhou, Y. Gao and L. Liu, *Zhongguo Niangzao*, 2010, **10**, 120.
9 W. Zhang, J. Hu, X. Liu and Y. Miao, *Faming Zhuanli Shenqing* 2014, CN103690427 A20140402.
10 S.N.A. Bukhari, I. Jantan, O. Unsal Tan, M. Sher, M. Naeem-u. Hassan and H.-L. Qin, *J. Agric. Food Chem.*, 2014, **62(24)**, 5538.
11 P. Maisuthisakul and M.H. Gordon, *J. Food Sci. Technol.*, 2014, **51(8)**, 1453.
12 E. Mendes, M.J. Perry and A.P. Francisco, *Expert Opin. Drug Discov.*, 2014, **9(5)**, 533.
13 Z. Chen, D. Cai, D. Mou, Q. Yan, Y. Sun, W. Pan, Y. Wan, H. Song and W. Yi, *Bioorg. Med. Chem.*, 2014, **22(13)**, 3279.
14 P. Fong, H.H.Y. Tong and C.M. Chao, C.M. *Nat. Prod. Commun.*, 2014, **9(2)**, 189.
15 M.R. Loizzo, R. Tundis and F. Menichini, Compreh. *Rev. Food Sci. S*, 2012, **11(4)**, 378.

16 Y. Wang, M.J. Curtis-Long, B.W. Lee, H.J. Yuk, D.W. Kim, X.F. Tan and K.H. Park, *Bioorg. Med. Chem.*, 2014, **22(3)**, 1115.
17 Y. Komori, M. Imai, T. Yamauchi, K. Higashiyama and N. Takahashi, *Bioorg. Med. Chem.*, 2014, **22(15)**, 3994.
18 I.E. Orhan and M.T. Hassan Khan, *Curr. Top. Med. Chem.*, 2014, **14(12)**, 1486.
19 N. Batra, S. Batra, A. Pareek and B.P. Nagori, *Int. Res. J. Pharm.*, 2012, **3(7)**, 24.
20 J. Liu, F. Wu, L. Chen, L. Zhao, Z. Zhao, M. Wang and S. Lei, *Food Chem.*, 2012, **135(4)**, 2872.
21 M.J. Matos, L. Santana, E. Uriarte, S. Serra, M. Corda, M.B. Fadda, B. Era and A. Fais, *J. Pharm. Pharmacol.*, 2012, **64**, 742.
22 Y. Masamoto, Y. Murata, K. Baba, Y. Shimoishi, M. Tada and K. Takahata, *Biol. Pharm. Bull.*, 2004, **27**, 422.
23 F. Sollai, P. Zucca, E. Sanjust, D. Steri and A. Rescigno, *Biol. Pharm. Bull.*, 2008, **31**, 2187.
24 L.-T.-T. Huong, G.M. Casanola-Martin, Y. Marrero-Ponce, A. Rescigno, L. Saso, V.S. Parmar, F. Torrens and C. Abad, *Mol. Divers.*, 2011, **15(2)**, 507.
25 A. Fais, M. Corda, B. Era, M.B. Fadda, M.J. Matos, E. Quezada, L. Santana, C. Picciau, G. Podda and G. Delogu, *Molecules*, 2009, **14**, 2514.
26 M.J. Matos, L. Santana, E. Uriarte, G. Delogu, M. Corda, M.B. Fadda, B. Era and A. Fais, *Bioorg. Med. Chem. Lett.*, 2011, **21**, 3342.
27 Y.M. Ha, S.W. Chung, S. Song, H. Lee, H. Suh and H.Y. Chung, *Biol. Pharm. Bull.*, 2007, **30**(9), 1711.
28 A.P. Oliveira Amorim, M.C. Campos de Oliveira, T. Azevedo Amorim and A. Echevarria, *Antioxidants*, 2013, **2**, 90.
29 P. Maisuthisakul and M.H. Gordon, *Food Chem.*, 2009, **117(2)**, 332.
30 G. Bargellini, *Alli II Congresso Naz. Chim. Pura Applicata*, 1926, 1295.
31 Y. Ming and D.W: Boykin, *Heterocycles*, 1987, **26(12)**, 3229.
32 M.J. Matos, C. Terán, Y. Pérez-Castillo, E. Uriarte, L. Santana and D. Viña, *J. Med. Chem.*, 2011, **54**, 7127.
33 N.R. Krishnaswamy, T.R. Seshadri and B.R. Sharma, *Ind. J. Chem.*, 1966, **4(3)**, 120.
34 B.B. Dey and K.K. Row, *Quarterly J. Ind. Chem. Soc.*, 1924, **1**, 107.
35 A. Sonn, *Berichte der Deutschen Chemischen Gesellschaft*, 1918, **51**, 821.
36 G. Bargellini, *Gazzetta Chimica Italiana*, 1927, **57**, 457.
37 I.C. Badhwar, W. Baker, B.K. Menon and K. Venkataraman, *J. Chem. Soc.*, 1931, 1541.
38 A.G. Taranto, A.L.B. Teles, J.Q. Araujo, B.A. Ferreira and M.Jr. Comar, *Rev. Ciênc. Farm. Básica Apl.*, 2012, **33(3)**, 437.
39 K. Hashimoto, A. Yamada, H. Hamano, S. Mori and H. Moriuchi, PCT Int. Appl. 1994, WO9424119 A119941027.
40 I. Kubo, I. Kinst-Hori, S.K. Chaudhuri, Y. Kubo, Y. Sànchez and T. Ogura, *Biorg. Med. Chem.*, 2000, **8**, 1749.
41 R. Re, N. Pellegrini, A. Proteggente, A. Pannala, M. Yang and C. Rice-Evans, *Free Rad. Biol. Med.*, 1999, **26**, 1231.
42 W. Yi, X. Wu, R. Cao, H. Song and L. Ma, *Food Chem.*, 2009, **117**, 381.
43 T. Mosmann, *J. Immunol. Methods*, 1983, **65**, 55.
44 Schrödinger package 2014-3, Schrödinger, LLC, New York, NY, 2014. Available: http://www.schrodinger.com (accessed December 2014).
45 W.T. Ismaya, H.J. Rozeboom, A. Weijn, J.J. Mes, F. Fusetti, H.J. Wichers and B.W. Dijkstra, *Biochemistry*, 2011, **50(24)**, 5477.
46 L.M. Kabeya, A.A. Marchi, A. Kanashiro, N.P. Lopes, C.H.T.P Silva, M.T. Pupo and Y.M. Lucisano-Valim, *Bioorg. Med. Chem.*, 2007, **15**, 1516.